Probing the Evolutionary Stages of Infrared Dark Cloud Cores

Vlas Sokolov[1], Vivien Chen[1], Sheng-Yuan Liu[2], Yu-Nung Su[2]

[1]Institute of Astronomy, National Tsing Hua University

[2]Institute of Astronomy & Astrophysics, Academia Sinica

Abstract

Infrared dark clouds (IRDCs) are cold and dense extinction feature found against the diffuse Galactic infrared emission, and are thought to be the potential sites for massive star formation. They often harbour dense cores in different evolutionary stages that are differentiated by various evolutionary tracers such as luminosity, temperature, line width, or CO depletion. In this study, we derive gas temperature of 12 IRDC cores to complete the last portion of a large deuterium fractionation survey of 44 IRDC cores. We adopt existing infrared classification based on *Spitzer*/IRAC 3-8μm colours and *Spitzer*/MIPS 24μm point-source emission to discuss evolutionary stages of the cores in terms of "quiescent", "intermediate", "active", and "red" types. We examine correlation between deuterium fractionation of N_2H^+ with several evolutionary tracers. A clear decreasing trend has been identified with gas temperature and line width.

Introduction

Studies of embedded core evolutionary sequence are crucial to understanding the initial conditions of star formation. Over the years, the infrared dark clouds (IRDCs), cold and dense molecular regions seen against the bright, diffuse infrared emission of the Galactic plane, have been shown to be promising sites for massive star formation in various evolutionary stages (Rathborne et al. 2006). Despite the important role of IRDCs in massive star formation, the chemistry of these objects is still poorly understood (Miettinen et al. 2011; Sanhueza et al. 2012). Several chemical clocks have been proposed to trace the evolution of cores embedded in infrared dark clouds. At the IRDC temperature regime, the gas-phase CO is thought to be depleted on dust grains, allowing for a signature prestellar chemical processes to occur. In particular, the enhancement of deuterated species takes place due to favourable temperature environment, and the gas-phase CO depletion on dust grains creates conditions for N_2D^+ abundance enrichment. $R_D(N_2H^+) \equiv N(N_2D^+) / N(N_2H^+)$, the deuterium fractionation of N_2H^+, has been shown before to be a dynamical age tracer in low-mass dense cores (Crapsi et al. 2005; Emprechtinger et al. 2009; Fontani et at. 2011). In previous studies (Chen et al. 2010, 2011), a number of protostellar cores has been studied, and a the use of deuterium fractionation as an evolutionary sequence tracer for high-mass cores has been suggested.

To investigate the relation of the deuterium fractionation trends to evolutionary stages of the IRDC cores, we have adopted infrared *Spitzer* IRAC/MIPS classification, first presented in Chambers et al. (2009). The cores are differentiated by *Spitzer* IRAC 3-8μm colours and the presence of *Spitzer* MIPS 24μm source. The "quiescent" type cores, tracing a starless phase of stellar evolution, are thought to evolve into the "intermediate" ones, followed by "active" type, which are likely to have embedded protostellar cores and an outflow activities associated with them. The cores bright in *Spitzer* IRAC 8um emission are considered as "red" type, possibly tracing the HII regions.

Observation and Data Analysis

The initial sample of 15 IRDC cores from Chen et al. (2011) of one IRDC and two HMPOs, initially selected to represent different stages of evolutionary sequence, was expanded with 17 IRDC cores from Rathborne et al. (2006) and Sakai et al. (2008). The sample was observed with Submillimeter Telescope for N_2H^+(3-2) N_2D^+(3-2) $C^{18}O$ (2-1) transitions.

In order to further increase the sample up to 44 cores, we present a measurement of ammonia emission in a sample of 14 cores in one high extinction cloud, G35.49-0.30, and two infrared dark clouds, G53.11+0.05 and G53.25+0.04. The ammonia spectra were taken on May 2012 with Nobeyama 45 meter radio telescope. Satellite components of (J,K) = (1,1) line were observed. The data were calibrated by NewStar package.

Figure 1 shows ammonia (1,1) inversion line fit, performed in CLASS package, and (2,2) line, approximated by a Gaussian since the satellite components of the line were not resolved. A method described by Bachiller et al. (1987) was used to derive the rotational temperatures of the infrared dark cloud cores in the sample. The results are listed in Table 1. The cores are found to have average temperatures about 14 K, comparable to 14-16 K for other IRDC studies (Sakai et at. 2008, Rygl et al. 2010).

Lastly, we used the infrared classification from Sanhueza et al. (2012) to classify half of our sample in terms of observable infrared properties, with two quiescent cores, four intermediate ones, twelve classified as active, and three red cores overlapping with the dark clouds used in this study.

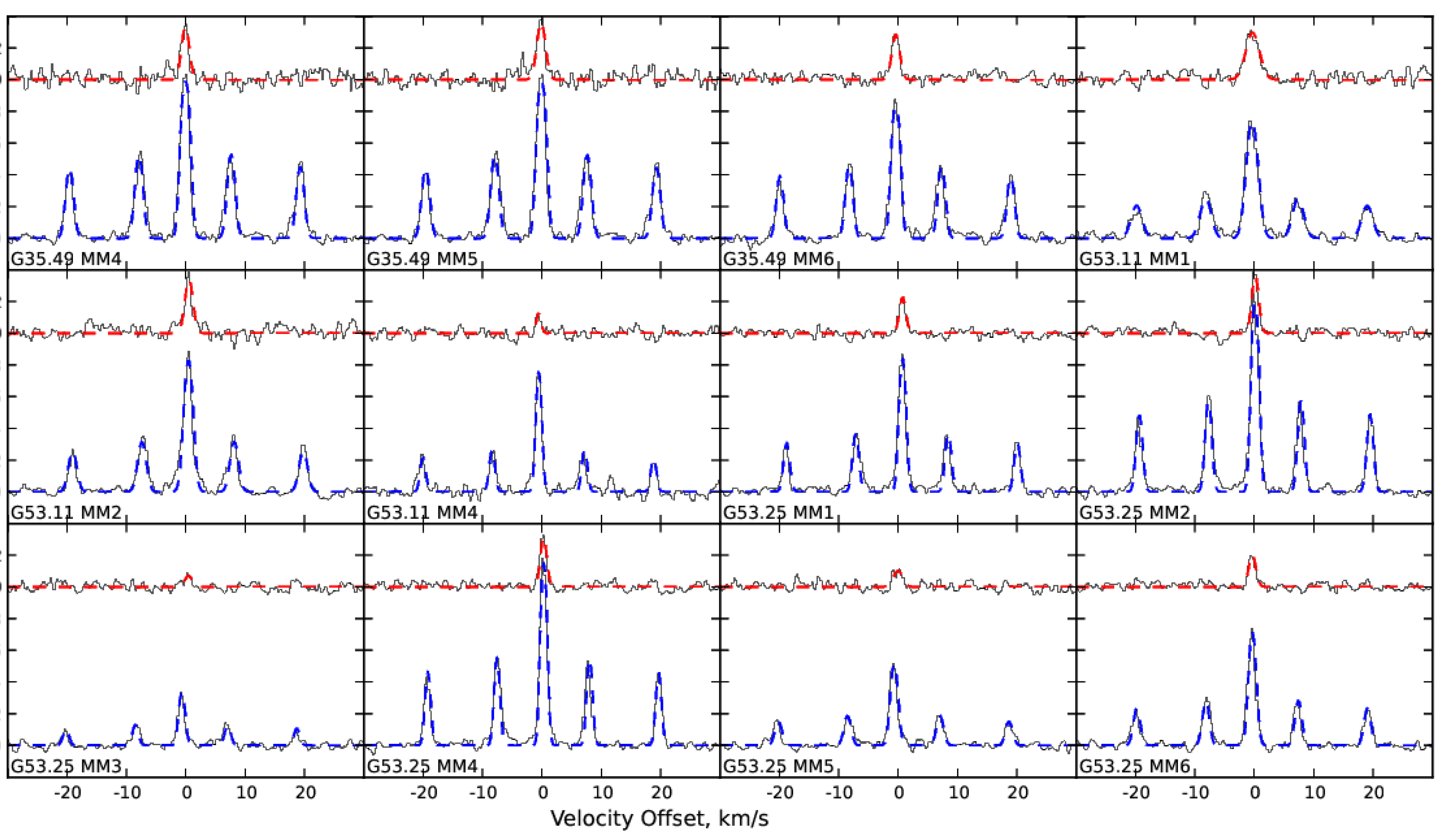

Figure 1. Spectral fits for the ammonia IRDC cores sample. G53.11 MM3 and MM5 are not included in this table, since the (J, K)=(2, 2) line was not detected for those sources.

Source	Main Group Opacity	(1,1) line width (km/s)	(2,2) line width (km/s)	T_{rot} (K)
G35.49 MM4	2.41 ± 0.08	1.44 ± 0.01	1.54 ± 0.12	13.0 ± 0.4
MM5	2.40 ± 0.07	1.45 ± 0.01	1.70 ± 0.12	13.8 ± 0.4
MM6	2.60 ± 0.12	1.33 ± 0.02	1.55 ± 0.10	13.2 ± 0.4
G53.11 MM1	0.62 ± 0.09	2.13 ± 0.04	2.67 ± 0.15	19.0 ± 1.3
MM2	0.97 ± 0.09	1.62 ± 0.03	1.56 ± 0.10	16.2 ± 0.8
MM4	0.71 ± 0.17	1.06 ± 0.04	0.93 ± 0.16	12.0 ± 1.1
G53.25 MM1	1.54 ± 0.10	1.16 ± 0.02	1.26 ± 0.09	13.4 ± 0.5
MM2	1.93 ± 0.07	1.20 ± 0.02	1.31 ± 0.06	13.3 ± 0.3
MM3	1.05 ± 0.22	1.11 ± 0.05	1.45 ± 0.32	14.0 ± 1.8
MM4	1.90 ± 0.08	1.06 ± 0.01	1.25 ± 0.06	13.3 ± 0.3
MM5	0.81 ± 0.12	1.35 ± 0.03	1.77 ± 0.26	14.2 ± 1.2
MM6	1.15 ± 0.08	1.30 ± 0.02	1.36 ± 0.10	14.2 ± 0.6

Table 1. Summary of ammonia spectral analysis; G53.11 MM3 and MM5 are not included in this table, since the (J, K)=(2, 2) line was not detected for those sources.

Results

Combined with the earlier results from Chen et al., 2011 the new sample agrees with the decreasing trend in deuterium fractionation against N_2H^+ line width and gas temperature (Figure 2). A decreasing behaviour of deuterium fractionation with $C^{18}O$ column density is also observed.

We suggest that the way to classify IRDC cores by their mid-infrared properties proposed by Chambers et al. (2009) can be used to relate the cores to their place in the embedded core evolutionary sequence. Figure 2 clearly shows that the cores characterised as "quiescent" and "intermediate" tend to have higher deuterium fractionation, lower gas temperatures, and larger line widths than the "active" and "red" types, as well the cores classified as HMSCs and HMPOs. The "active" type cores are scattered in the parameters discussed here, but their mean value positions are within their proposed evolutionary place. The trend of decreasing deuterium fractionation with evolution does not seem to extend to the quiescent type when compared the intermediate one. Similar behaviour of N_2H^+/HCO^+ abundance ratio was reported in Sanhueza et al. (2012).

Our study suggests a general behaviour of deuterated species in high-mass protostellar cores in relation to their evolutionary stages, in particular the use of $R_D(N_2H^+)$ as a chemical clock for high-mass protostellar objects.

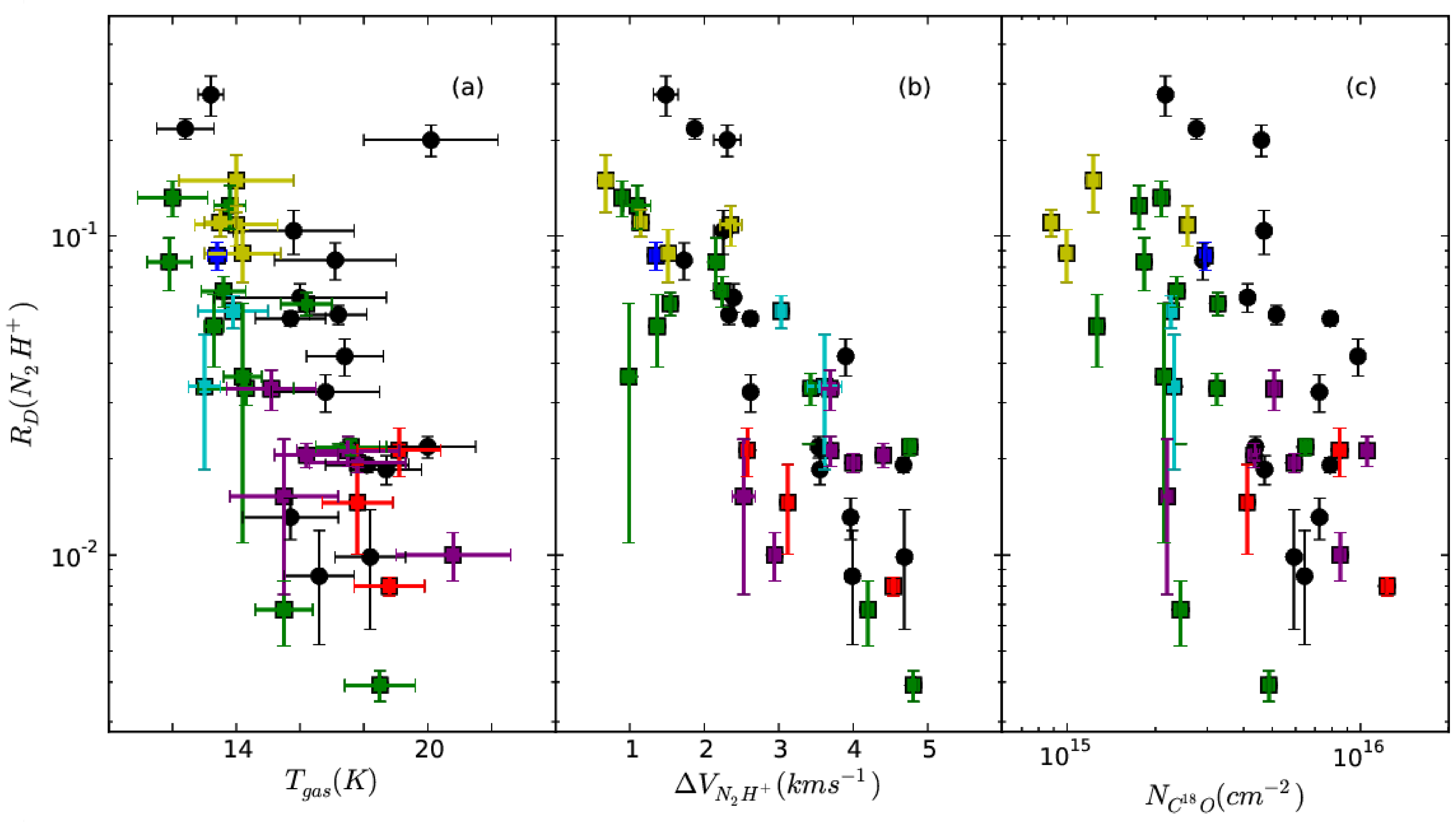

Figure 2. (a) Deuterium fractionation, $R_D(N_2H^+)$, vs. gas temperature, T_{gas}. The coloured squares indicate evolutionary stages of the cores: cyan for the cores classified as "quiescent", yellow for "intermediate" cores, green for "active" objects, and "red" type cores are plotted as red squares; cores in purple are IRAS 18151—1208 and IRAS 18223—1243 cores that are HMPOs and HMSCs; black is reserved for objects that were not previously classified. (b) $R_D(N_2H^+)$ vs fitted line width, $\Delta v(N_2H^+)$. (c) $R_D(N_2H^+)$ vs $C^{18}O$ column density.

References

Bachiller, R., Guilloteau, S., & Kahane, C. 1987, A&A, 173, 324

Chen, H.-R., Liu, S.-Y., Su, Y.-N., & Wang, M.-Y. 2011, ApJ, 743, 196

Chen, H.-R., Liu, S.-Y., Su, Y.-N. 2013, IAU Symp, 292, in press

Chambers, E. T., Jackson, J. M., Rathborne, J. M., & Simon, R. 2009 ApJS, 181, 360

Crapsi, A., Caselli, P., Walmsley, C. M., Myers, P. C., Tafalla, M., Lee, C. W., & Bourke, T. L. 2005, ApJ, 619, 379

Emprechtinger, M., Caselli, P., Volgenau, N. H., Stutzki, J., & Wiedner, M. C. 2009, A&A, 493, 89

Fontani, F., Palau, A., Caselli, P., et al. 2011, A&A, 529, L7

Ho, P. T. P., & Townes, C. H. 1983, ARA&A, 21, 239

Miettinen, O., Hennemann, M., & Linz, H. 2011, A&A, 534, A134

Rathborne, J. M., Jackson, J. M., & Simon, R. 2006, ApJ, 641, 389

Rygl, K. L. J., Wyrowski, F., Schuller, F., Menten, K. M., 2010, A&A, 515, 42

Sakai, T., Sakai, N., Kamegai, K., et al. 2008, ApJ, 678, 1049

Sanhueza, P., Jackson, J. M., Foster, J. B., Garay, G., Silva, A. & Finn, S. C. 2012 ApJ, 756, 60